analytical chemistry

Article

pubs.acs.org/ac

Investigating Catalase Activity Through Hydrogen Peroxide Decomposition by Bacteria Biofilms in Real Time Using Scanning Electrochemical Microscopy

Erwin Abucayon,[†] Neng Ke,[†] Renaud Cornut,[‡] Anthony Patelunas,[§] Douglas Miller,[§] Michele K. Nishiguchi,[§] and Cynthia G. Zoski*,[†]

[†]Department of Chemistry and Biochemistry, New Mexico State University, Las Cruces, New Mexico 88003, United States

[‡]Laboratoire de Chimie des Surfaces et Interfaces, Gif-sur-Yvette, France

[§]Department of Biology, New Mexico State University, Las Cruces, New Mexico 88003, United States

Supporting Information

ABSTRACT: Catalase activity through hydrogen peroxide decomposition in a 1 mM bulk solution above *Vibrio fischeri* (*γ-Protebacteria-Vibrionaceae*) bacterial biofilms of either symbiotic or free-living strains was studied in real time by scanning electrochemical microscopy (SECM). The catalase activity, in units of micromoles hydrogen peroxide decomposed per minute over a period of 348 s, was found to vary with incubation time of each biofilm in correlation with the corresponding growth curve of bacteria in liquid culture. Average catalase activity for the same incubation times ranging from 1 to 12 h was found to be 0.28 ± 0.07 μmol H_2O_2/min for the symbiotic biofilms and 0.31 ± 0.07 μmol H_2O_2/min for the free-living biofilms, suggesting similar catalase activity. Calculations based on Comsol Multiphysics simulations in fitting experimental biofilm data indicated that approximately (3 ± 1) × 10^6 molecules of hydrogen peroxide were decomposed by a single bacterium per second, signifying the presence of a highly active catalase. A 2-fold enhancement in catalase activity was found for both free-living and symbiotic biofilms in response to external hydrogen peroxide concentrations as low as 1 nM in the growth media, implying a similar mechanism in responding to oxidative stress.

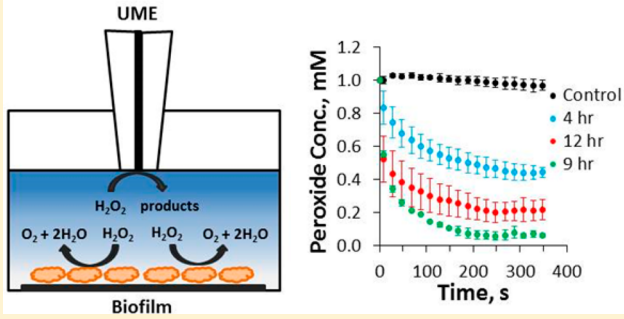

We report the use of scanning electrochemical microscopy (SECM) in investigating catalase activity, a defense mechanism of many bacteria, at the surface of biofilms of the bioluminescent marine bacterium *Vibrio fischeri* (*V. fischeri*). Understanding the processes by which beneficial (i.e., mutualistic) and pathogenic bacteria successfully colonize host tissues is a major goal in biology and biomedicine.[1−8] *V. fischeri* is a beneficial bacterium found within the symbiotic light-emitting organs of sepiolid squids and monocentrid fishes (Mollusca: Cephalopoda). This unique system is used as an experimental model because the natural occurrence between *Vibrio* bacteria and specific host tissues can be used to explore the stages by which such associations develop as well as the mechanisms underlying specificity and host signaling without confounding effects typically observed in the presence of multiple bacterial species.[9] Sepiolid squids are nocturnal predators that hide during the day but emerge each night to forage in the water column for prey. The luminous, gram-negative *V. fischeri* colonize the squid's internal light-emitting organ and generate bioluminescence, which provides a camouflage strategy termed counterillumination that enables the squid to match downwelling moonlight by silhouette reduction.[10] In return, *V. fischeri* bacteria receive nutrients from the squid host.[11] This mutualistic relationship is the basis for a continuing and long-term symbiosis.

All host animals instinctively protect themselves against colonization by inappropriate or pathogenic microorganisms. A central theme in bacteria−host interactions is that the symbiont either avoids damage by host immune defenses and/or communicates with host cells to modulate or regulate them.[12−20] Both mechanisms may contribute to symbiont specificity and are used in the *V. fisheri*-squid symbiosis. One of these multiple selective mechanisms is the imposition of oxidative stress, where oxygen is partially reduced by a squid-activated-membrane oxidase complex to produce hydrogen peroxide.[21] The hydrogen peroxide reacts with squid-produced halide peroxidase to generate hypochlorous acid, a known bactericide. *V. fischeri* bacteria counteract this oxidative stress through the presence of a highly active catalase in their periplasm. The catalase rapidly reduces the effective concentration of hydrogen peroxide (i.e., through decomposition to water and oxygen) near bacteria cell surfaces.[16−18,22] Other

Received: August 5, 2013
Accepted: December 13, 2013
Published: December 13, 2013

symbiotic associations make use of catalase to eliminate host generated hydrogen peroxide during colonization, such as microbes in nasal cavities,[23] plant roots,[24] and in soil where fungi produce peroxide to compete against other organisms.[25] Some bacteria have developed high catalase activity in order to adapt to extreme hydrogen peroxide environments such as encountered in processing plants where hydrogen peroxide is used as a bleaching agent.[26−28] Catalase activity has also been reported for pathogenic bacteria which coexist with hydrogen peroxide producing beneficial bacteria in oral polymicrobial systems.[29] Therefore, current understanding of damage and defense due to oxidative stress continues to be a topic of great interest and has largely been pioneered through studies in *E. coli*.[30]

Catalase is also responsible for the decomposition of hydrogen peroxide produced as a byproduct of oxygen metabolism, and its activity has been found to vary during the bacteria growth cycle.[22,31] For example, catalase activity was enhanced more than 3-fold in planktonic *V. fischeri* cells approaching stationary phase.[22] Addition of micromolar hydrogen peroxide during early logarithmic growth resulted in a 4-fold increase in activity.[22] *V. fischeri* catalase expression has been reported to be controlled by a single catalase gene, *katA*. Kat A is the predominantly expressed catalase enzyme whether hydrogen peroxide is produced internally through metabolic processes or externally from a host.[22] *katA* is also common in many bacteria and is responsible for their catalase expression.[5] Other bacteria, such as *E. coli*, induce a catalase as a result of oxidative stress that is distinct from a separate catalase induced at stationary phase.[30]

Catalase activity is most commonly determined quantitatively using spectroscopy[22,31−33] or Clark-type electrodes[34] to measure hydrogen peroxide decomposition in planktonic cell extracts. It is also measured qualitatively by judging the degree of bubbling due to the addition of hydrogen peroxide to bacteria cells.[22,35] These methods lack the ability to quantify local hydrogen peroxide concentration at the surface of a biofilm. Here we report the use of SECM[36,37] to investigate catalase activity through the change in hydrogen peroxide concentration as a function of time due to its decomposition at the surface of *V. fischeri* biofilms. In SECM, a sensing tip (i.e., an ultramicroelectrode (UME) of size 10−25 μm diameter) is positioned above a substrate through a feedback approach curve (i.e., tip current, i_T, vs distance, d, where d is scanned in the z direction to a fixed position above a substrate such as a biofilm) and measures the local transient hydrogen peroxide concentration over the biofilm in response to its catalase activity.[38] This allows the effective concentration of hydrogen peroxide above a biofilm to be measured *in situ*. We also investigate catalase activity as a function of incubation time of the biofilm and relate this activity to the growth curve of planktonic bacteria. Furthermore, we demonstrate that catalase activity increases in biofilms exposed to hydrogen peroxide concentrations ranging from nM to μM early in the logarithmic phase of growth. Both symbiotic and free-living strains (i.e., cannot infect sepiolid squids but do co-occur) of *V. fischeri* bacteria were studied in order to determine if differences exist in their catalase activity. Electrochemical measurements of hydrogen peroxide concentration have been reported in several studies,[39−45] but none have dealt with hydrogen peroxide decomposition and its relationship to catalase activity as a function of biofilm incubation and increased activity during biofilm growth and on external exposure to hydrogen peroxide during early logarithmic growth. SECM is increasingly being applied to biological systems to measure local concentration over soft biological samples and for imaging.[46−49] For example, SECM was recently used in real-time mapping of local hydrogen peroxide production across a biofilm of oral bacteria and in observing its consumption in a polymicrobial biofilm through a mechanism involving one of the bacteria during spatial scanning,[50] in the discovery of a biofilm electrocline (i.e., of oral bacteria) using real-time 3D metabolite analysis,[51] and in assessing multidrug resistance on cell coculture patterns.[52]

EXPERIMENTAL SECTION

Chemicals. Artificial seawater (Instant Ocean), tryptone (Difco), yeast extract (Difco), glycerol (Sigma), agar (Difco), $MgSO_4{\cdot}7H_2O$ (Fisher Scientific), $CaCl_2{\cdot}2H_2O$ (Fisher Scientific), NaCl (Fisher Scientific), KCl (Fisher Scientific), K_2HPO_4 (Fisher Scientific), NH_4Cl (Fisher Scientific), Tris-HCl (Fisher Scientific), H_2O_2 (Fisher Scientific, 30%).

Media. Bacteria strains were grown in SWT (Seawater-tryptone) media, containing 70% artificial seawater, 0.5% tryptone, 0.3% yeast extract, and 0.3% glycerol. DMM (Defined minimal media, pH 8.0) contained 12.3 g/L $MgSO_4{\cdot}7H_2O$, 1.47 g/L $CaCl_2{\cdot}2H_2O$, 17.5 g/L NaCl, 0.745 g/L KCl, 58.1 g/L K_2HPO_4, 1.0 g/L NH_4Cl, and 3 mL/L glycerol in 50 mM Tris-HCl (pH 7.9). SWT agar plates contained 1.5% agar.

Bacteria Growth Curves. Two wild type *V. fischeri* strains, collected by M.K.N., were used: CB37 (free-living, collected in Australia (Coogee Bay, New South Wales)); ETBB10-1 (symbiotic from *Euprymna tasmanica* squid, collected in New South Wales, Australia (Botany Bay)). *V. fischeri* were cultured overnight in 50 mL of SWT media from cultured freezer stocks stored at −80 °C. The overnight cell suspension (in triplicate) was diluted to an absorbance of 0.3 with SWT. Subcultures contained 1 mL of each diluted overnight suspension inoculated into 200 mL of fresh SWT media. A control flask of 1 mL of SWT in 200 mL of fresh SWT was also prepared. All incubations were performed in a New Brunswick Scientific Excella E25 Incubatore/Shaker programmed at 28 °C, 250 rpm. Volumes of 1 mL were taken from each flask, and absorbance was measured on a ThermoScientific BioMate 3 spectrophotometer at 600 nm at selected times (12 h for *V. fischeri* CB37 and 24 h for *V. fischeri* ETBB10-1).

Biofilm Formation. Overnight cultures (in triplicate) of *V. fischeri* were grown in 50 mL of SWT media from cultured freezer stocks stored at −80 °C. Subcultures contained 1 mL from each overnight culture and placed in 50 mL SWT; bacteria subcultures were incubated to an absorbance (600 nm) of 0.3. All incubations were performed in a New Brunswick Scientific Excella E25 Incubatore/Shaker programmed at 28 °C, 250 rpm; absorbance was measured on a ThermoScientific BioMate 3 spectrophotometer at 600 nm. Cells were pelleted at 2500 rpm for 20 min by centrifugation (Sorvall Legend RT Centrifuge) and resuspended in SWT media to an absorbance (600 nm) of 1.5. The cell suspension (100 μL) was spread on a glass coverslip (Thomas Scientific, #1.5, 18 mm diameter) laid on a freshly prepared SWT agar plate using a bent glass rod. Each coverslip was incubated for 10 min at 28 °C to allow bacteria attachment and then transferred to a fresh Petri dish (VWR Polystyrene, 35 mm × 10 mm, Falcon Easy Grip) containing 500 μL of SWT and incubated at 28 °C under static conditions for specific incubation times ranging from 1 to 24 h. Four coverslips were prepared from each cell suspension for each incubation time. For incubations greater than 6 h, 500 μL

dx.doi.org/10.1021/ac402475m | *Anal. Chem.* 2014, 86, 498−505

of fresh SWT was added as follows: for 9 and 12 h incubations, at 6 h into the incubations; for 24 h incubations, at 6 h, at 12 and 18 h (500 μL of media removed and 500 μL of fresh SWT added). After incubation, each biofilm coverslip was rinsed with SWT by careful dipping three times. The back of each coverslip was dried with Kim Wipes and secured in a fresh Petri dish (VWR Polystyrene, 35 mm × 10 mm, Falcon Easy Grip) with double sided tape (3M) and used in the SECM experiments described below. Each series of incubations for each bacterial strain were repeated with three separate overnight cultures on three separate days.

Electrodes and Electrochemical Cell. Pt wire (10 μm diameter, 99.99% hard, Goodfellow) was used in fabricating ultramicroelectrode (UME) SECM tips, as described elsewhere.[53,54] The SECM tips used in these experiments were shaped to RG = 3, where RG is the ratio between the SECM tip diameter and the diameter of the active UME surface. Prior to use, all SECM tips were polished with 0.05 μm alumina on microcloth pads (Buehler, Lake Bluff, IL) and cycled in 0.1 M H_2SO_4 in the potential range from −0.55 to 0.6 V vs Ag/AgCl, at 0.1 V/s for 80 cycles to a constant cyclic voltammogram. Pt wire (0.5 mm diameter, 99.99%, as drawn, Goodfellow) was used as the counter electrode, and the reference electrode was Ag/AgCl (satd).

The electrochemical cell consisted of a Petri dish (VWR Polystyrene, 35 mm × 10 mm, Falcon Easy Grip) with the biofilm coverslip secured at the bottom center with double sided tape (3M). A solution of 2.5 mL of DMM spiked with H_2O_2 to a concentration of 1 mM was used.

Instrumentation. A CHI 900 SECM (CH Instruments, Texas) coupled with a home-built Faraday cage on a vibration table (VH3030W-OPT, Newport) was used in all SECM experiments. UMEs were characterized and cleaned electrochemically using a CHI 760 D potentiostat (CH Instruments, Texas).

SECM Experiments. The SECM tip was positioned using previously reported procedures.[37] An approach curve (tip current, i_T vs distance, d) was recorded above the biofilm immersed in 2.5 mL of DMM using oxygen as a mediator by holding the tip potential E_T at −0.47 V vs Ag/AgCl (satd.). The distance between tip and biofilm was then fixed at 100 μm above the biofilm in order to avoid effects from the biofilm topography, while still being able to record the current vs time transient for the hydrogen peroxide decomposition.

A background chronoamperometric curve was recorded in the absence of hydrogen peroxide at the same height by pulsing the tip at 0.65 V for 10 s and reversing to 0.15 V for 10 s as shown in Figure S1 in the Supporting Information; the duration of the potential pulse sequence was 360 s, with the last measurement time at 348 s at E_T = 0.65 V. The DMM was then spiked with hydrogen peroxide while stirring toward the end of the 5 s quiet time in order to ensure a uniform final concentration of 1 mM. The current due to hydrogen peroxide oxidation was measured as a function of time during each tip potential pulse at E_T = 0.65 V. This potential pulse was followed by another at E_T = 0.15 V for 10 s in order to electrochemically clean the UME surface. The current at 8 s during each 10 s pulse at 0.65 V was background subtracted and converted to H_2O_2 concentration using calibration curves similar to that shown in Figure S2 in the Supporting Information. Calibration curves were recorded over bare coverslips at peroxide concentrations ranging from 0.2 to 1.2 mM and under identical conditions as the biofilm experiments. The current vs time curves and the concentration vs time curves corresponding to each incubation time were averaged for each of the three separate overnight subcultures. Control experiments in the presence and absence of hydrogen peroxide were performed over a bare, glass coverslip for comparison.

RESULTS AND DISCUSSION

Figure 1 shows the schematic of the experimental setup in which a SECM tip positioned 100 μm above a biofilm monitors

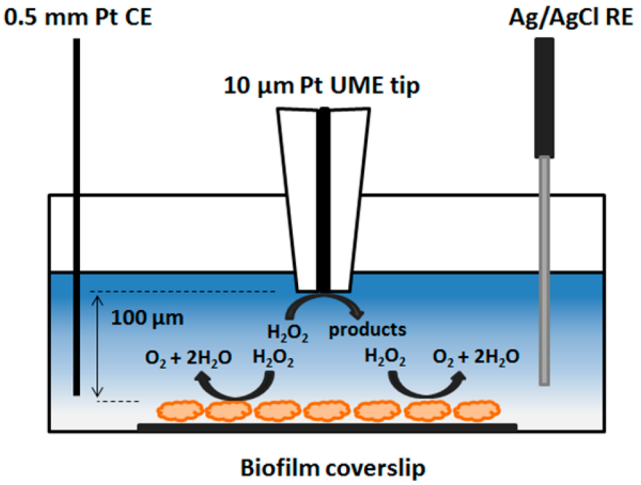

Figure 1. Schematic of the electrochemical experimental setup for SECM real-time measurement of hydrogen peroxide decomposition by a bacterial biofilm.

the hydrogen peroxide concentration gradient that develops with time in the electrochemical cell as a bulk solution of 1 mM hydrogen peroxide is decomposed at a biofilm surface. The decomposition of hydrogen peroxide by *V. fischeri* CB37 (free-living) and *V. fischeri* ETBB10-1 (symbiotic) biofilms as a function of incubation time (e.g., CB37, 1−12 h; ETBB10-1, 1−24 h) are shown in Figures 2a and 3a, respectively. Each concentration point in the graphs corresponds to the chronoamperometric current due to hydrogen peroxide oxidation at a particular time (e.g., t = 8 s during a series of 10 s pulses over a period of 348 s) as shown in the corresponding current vs time plots in Figures S3 and S4 in the Supporting Information and calculated using calibration curves similar to that shown in Figure S2 in the Supporting Information. The error bars in Figures 2a and 3a and Figures S3 and S4 in the Supporting Information were calculated based on three independent bacteria overnight and subcultures and at least three independent measurements within each subculture for each *V. fischeri* strain. Control experiments over bare glass coverslips were recorded in the presence of 1 mM hydrogen peroxide and showed little decrease in peroxide concentration over the duration of the experiment compared to those in the presence of a biofilm as shown in the figures.

For the *V. fischeri* CB37 and ETBB10-1 biofilms, the hydrogen peroxide concentration initially decreased from a bulk concentration of 1 mM to quasi-steady-state concentrations (i.e., corresponding to increasingly less negative currents in Figures S3 and S4 in the Supporting Information). The initial decay and the final quasi-steady-state hydrogen peroxide concentrations were found to be related to the incubation time of the individual biofilms and to the *V. fischeri* strains. Decreasing hydrogen peroxide concentration detected at the

dx.doi.org/10.1021/ac402475m | *Anal. Chem.* 2014, 86, 498−505

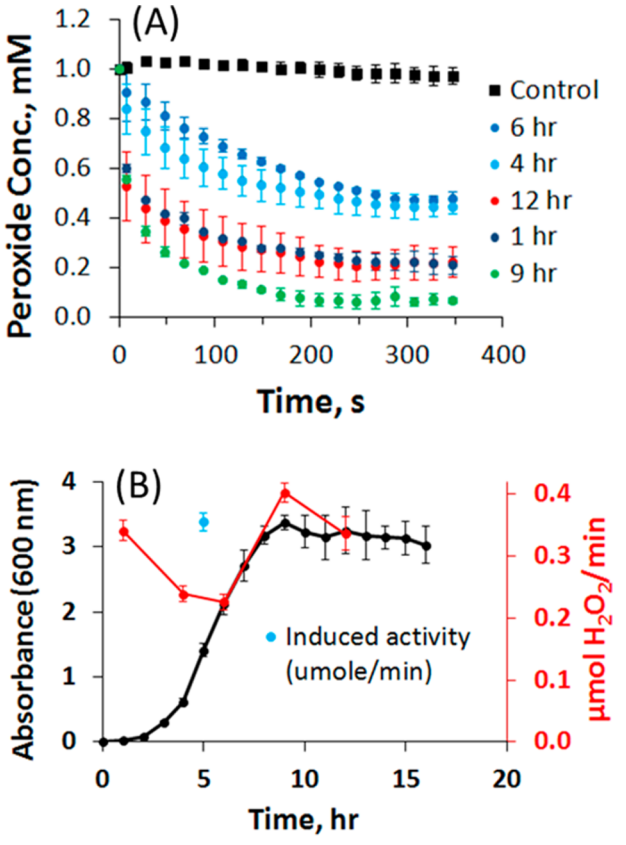

Figure 2. Hydrogen peroxide decomposition activity on *V. fischeri* CB37 biofilms at different incubation times. (A) Hydrogen peroxide concentration vs time curves generated from the corresponding current vs time curves (Figure S3 in the Supporting Information). (B) Comparison of growth curve (left axis, black line and solid dots) for planktonic *V. fischeri* CB37 bacteria and hydrogen peroxide decomposition activity (right axis, red line, and solid dots) on *V. fischeri* CB37 biofilms at designated incubation times. Decomposition activity represents the difference between initial and quasi-steady H_2O_2 moles divided by the analysis time of 348 s. Error bars represent standard deviation based on three independent measurements of each of three overnight cultures. The solid blue dot corresponds to incubation with 10 μM hydrogen peroxide at 4 h and measurement of induced activity at 5 h.

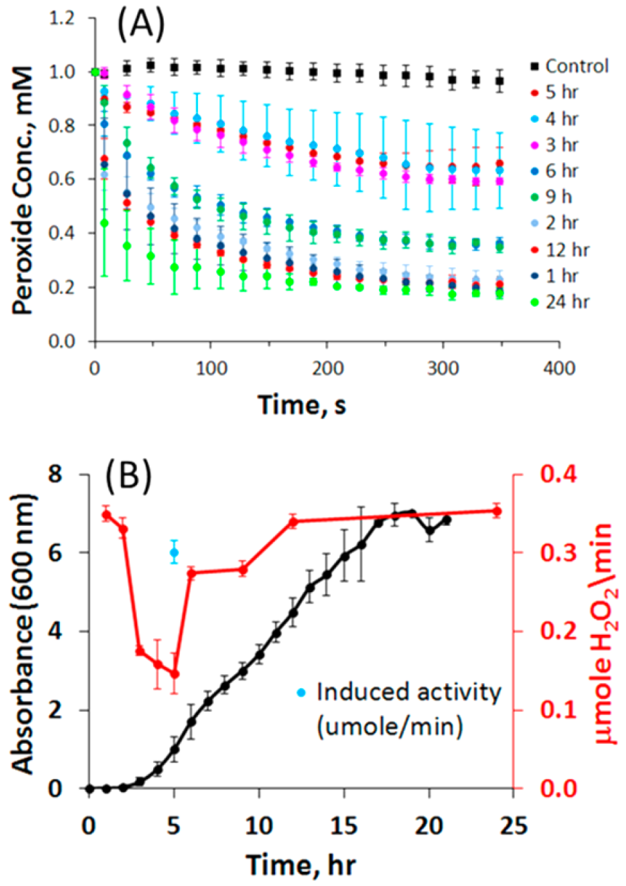

Figure 3. Hydrogen peroxide decomposition activity on *V. fischeri* ETBB biofilms at different incubation times. (A) Hydrogen peroxide concentration vs time curves generated from the corresponding current vs time curves (Figure S4 in the Supporting Information). (B) Comparison of growth curve (left axis, black line and solid dots) for planktonic *V. fischeri* ETBB10-1 bacteria and hydrogen peroxide decomposition activity (right axis, red line and solid dots) at *V. fischeri* ETBB10-1 biofilms at designated incubation times. Decomposition activity represents the difference between initial and quasi-steady H_2O_2 moles divided by the analysis time of 348 s. Error bars represent standard deviation based on three independent measurements of each of three overnight cultures. The solid blue dot corresponds to incubation with 10 μM, 10 nM, and 1 nM hydrogen peroxide at 4 h and measurement of induced activity at 5 h. Error bars represent standard deviation based on three independent measurements of each of three overnight cultures for each peroxide concentration.

SECM tip indicated increased hydrogen peroxide decomposition activity at the surface of the biofilm. We attribute this activity to the presence of catalase in the bacteria of the biofilm.

Correlation of Biofilm Peroxide Decomposition With Planktonic Bacteria Growth Curves. Figure 2A shows the change in the hydrogen peroxide concentration vs time in the presence of *V. fischeri* CB37 biofilms at different stages of incubation. In comparison, the control curve in the absence of *V. fischeri* CB37 biofilm demonstrates that the hydrogen peroxide concentration did not change significantly from the 1 mM bulk concentration over the measurement time. In the presence of the biofilms at different stages of incubation, there was a decrease in hydrogen peroxide concentration in the vicinity of the tip which was found to vary in three general incubation groups (i.e., 6, 4 h, and 12, 1 h, and 9 h) according to the growth stages of the bacteria. Figure 2B shows the growth curve of planktonic *V. fischeri* CB37, recorded as absorbance (600 nm) vs time, at hourly intervals over 16 h. This growth curve features a lag time in growth up to approximately 2 h, a log phase growth between 3 and 9 h and stationary growth after 10 h. Figure 2B also exhibits variation in hydrogen peroxide decomposition activity, expressed in units of micromoles hydrogen peroxide decomposed per minute (i.e., the difference between the initial and quasi-steady H_2O_2 moles divided by the analysis time of 348 s), which was calculated from the hydrogen peroxide concentration vs time curves (Figure 2A). Similar units have been used in previous discussions of catalase activity in planktonic *V. fischeri* bacteria where one U of catalase activity corresponds to 1 μmol of hydrogen peroxide decomposed per minute or, more generally, as U/mg catalase protein or U/cell.[22,55] Here, we similarly correlate hydrogen peroxide decomposition with catalase activity in *V. fischeri* biofilms. Early decrease in catalase activity from 1 h (lag phase) to 4 h incubation (log phase) can be attributed to dilution of catalase as the number of bacteria cells increases without a corresponding increase in catalase synthesis.

dx.doi.org/10.1021/ac402475m | *Anal. Chem.* 2014, 86, 498−505

During this time, existing catalase is divided between two daughter cells during each division.[31] The *V. fischeri* CB37 biofilm formed during 1 h incubation (i.e., lag phase) was found to decompose hydrogen peroxide more efficiently than biofilm formed from 4 h incubations (i.e., log phase, Figure 2A). Similarly, catalase activity of *V. fischeri* CB37 biofilm formed during 6 h incubation (log phase) was only slightly lower than that formed during the 4 h incubation. There was an increase in the catalase activity as the incubation time for the *V. fischeri* CB37 biofilms approached the stationary phase of the *V. fischeri* CB37 growth curve, reaching maximum activity at 9 h incubation (i.e., end of log phase). This decrease in catalase activity during the log phase and increase on approach to the stationary phase has been reported for other planktonic *V. fischeri* strains, where catalase activity was determined in cell extracts of bacteria measured at different times during its growth in rich media with shaking.[22,26−28,31]

Figure 3A shows the change in the hydrogen peroxide concentration vs time in the presence of *V. fischeri* ETBB10-1 biofilms at different incubation times over 24 h. Similar to *V. fischeri* CB37, the presence of *V. fischeri* ETBB10-1 biofilms produced a decrease in hydrogen peroxide concentration in the vicinity of the tip, which varied according to growth stages of the planktonic bacteria. Figure 3B shows the growth curve for planktonic *V. fischeri* ETBB bacteria, recorded as absorbance (600 nm) vs time over 21 h. This growth curve shows that planktonic *V. fischeri* ETBB10-1 develop through two log phases and two semistationary phases before reaching a stable stationary phase at approximately 16 h incubation. In general, the growth curve features a lag time in growth up to about 2 h, log phase growth between 3 and 7 h, semistationary growth between 7 and 10 h, a second log phase growth between 10 and 13 h, and a second semistationary growth starting at 13 h, followed by stationary growth at about 17 h. The two separate log phase periods feature a similar slope that is steeper than the two semistationary slopes, which are also similar to each other. Figure 3B also shows the variation in catalase activity (i.e., expressed as micromoles of hydrogen peroxide decomposed per minute) calculated from hydrogen peroxide concentration vs time curves in Figure 3A at different incubation times and its correlation with the growth curve. There is a dramatic decrease in catalase activity from one and two hour incubation (lag phase) to three hour incubation (log phase), followed by a steady decrease in activity from 3 to 5 h incubation (log phase). At 6 h incubation (log phase) corresponding to the entry into the first semistationary phase, the *V. fischeri* ETBB10-1 biofilm shows a dramatic increase in catalase activity, followed by a slight decrease in activity at 9 h incubation corresponding to the second log phase. The *V. fischeri* ETBB10-1 biofilm shows increased activity at 12 h incubation corresponding to the entry into the second semistationary phase, where the activity is approximately maintained through 24 h incubation (i.e., stationary phase).

V. fischeri ETBB10-1 biofilms show catalase activity comparable to those of *V. fischeri* CB37 up to 5 h incubation. At 6 h incubation, *V. fischeri* ETBB10-1 biofilms show slightly higher catalase activity due to entry into the first semistationary growth phase in comparison to *V. fischeri* CB37 biofilms which are still in the log phase of growth. At 9 h incubation, *V. fischeri* ETBB10-1 biofilms begin a second log phase growth with a corresponding decrease in catalase activity compared to *V. fischeri* CB37 biofilms, which are entering the stationary growth phase. *V. fischeri* ETBB10-1 biofilms enter a second semistationary growth phase at 12 h incubation with catalase activity comparable to that of *V. fischeri* CB37 now in the stationary phase. Overall, the average catalase activity for the common incubation times of 1, 4, 6, 9, and 12 h was found to be 0.28 ± 0.07 μmol H_2O_2/min for the symbiont (i.e., *V. fischeri* ETBB10-1) compared to 0.31 ± 0.07 μmol H_2O_2/min for the free living (i.e., *V. fischeri* CB37) *V. fischeri* biofilms suggesting that catalase activity is similar for both the *V. fischeri* CB37 and ETBB10-1 biofilms, despite differences in the planktonic growth curve behavior as well as life history strategy (i.e., free-living versus symbiotic).

Catalase activity of the *V. fischeri* ETBB10-1 and CB37 biofilms measured using SECM can be compared to those reported for various planktonic *Vibrio* species from different hosts and geographic locations, where the activities were measured using spectroscopy and reported in units of μmol H_2O_2 decomposed/min/cell.[55] Such comparisons are of interest from an evolutionary standpoint since different *Vibrio* bacteria encompass a variety of life history strategies (e.g., free-living, beneficial, pathogenic, commensal, saprophytic) and may have specific uses for catalase besides fending off immune response from a particular host. Examples include *V. fischeri* (host: fish, shrimp; Black Sea) with catalase activities ranging from 1 to 2 × 10^{-7}, *Vibrio harveyi* (host: mussel; Black Sea) with activities ranging from 4 to 7 × 10^{-8}, and *Vibrio sp.* (host: mollasc, fish, shrimp, free living; Black and Azov Seas) with activities ranging from 4 to 8 × 10^{-8}. In comparison, catalase activities for *V. fischeri* ETBB10-1 (host: squid; Botany Bay, Australia) and *V. fischeri* CB37 (free living; Coogie Bay, Australia) biofilms from Figures 2 and 3, respectively, in this work ranged from 2 to 5 × 10^{-9} μmol H_2O_2 decomposed/min/cell (i.e., based on bacteria cell density = 3.5 × 10^7/cm^2 and coverslip area of 2.54 cm^2), which are within 2 orders of magnitude of the planktonic values. Differences in catalase activity can be attributed to several factors including geographic location, type of host, cell density, and planktonic (i.e., the reported activities[55]) vs biofilm (i.e., our work) catalase activity, in addition to methodology (i.e., spectroscopy vs SECM).

Figure 4 shows fitted simulated (solid lines) curves which demonstrate that hydrogen peroxide concentration gradients that developed between the biofilm surface and the SECM tip could be fit to the experimental response (solid dots) by the biofilms upon exposure to 1 mM hydrogen peroxide. Although

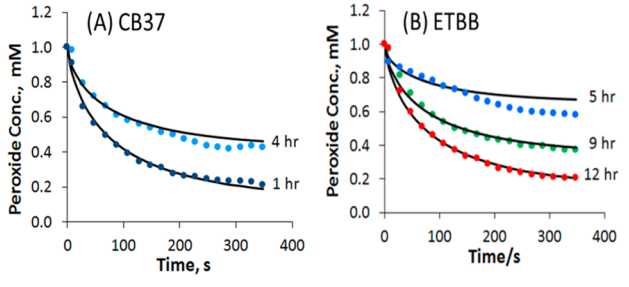

Figure 4. Comparison of simulated (solid black lines) and experimental (solid colored dots) of hydrogen peroxide concentration vs time curves at *V. fischeri* biofilms of CB37 (A) and ETBB10-1 (B) bacteria with an SECM tip located 100 μm above the biofilm surface. The diameter of the SECM tip was 10 μm (RG = 3). Simulated curves were generated with fluxes of (A) CB37: 1.6 × 10^{-10} mol/cm^2 s (4 h) and 2.5 × 10^{-10} mol/cm^2 s (1 h); (B) ETBB10-1: 0.9 × 10^{-10} mol/cm^2 s (5 h), 1.8 × 10^{-10} mol/cm^2 s (9 h), and 2.4 × 10^{-10} mol/cm^2 s (12 h) biofilms.

dx.doi.org/10.1021/ac402475m | *Anal. Chem.* 2014, 86, 498−505

SECM is a very useful method for measuring the local concentration of hydrogen peroxide above the biofilm or 100 μm from the biofilm surface, as previously discussed, it does not give the concentration or flux at the biofilm surface. Digital simulations can be used to determine the exact hydrogen peroxide flux at the biofilm surface in SECM experiments when the tip−substrate distance is known. Key parameters of the simulation model are given in the Supporting Information. The simulation assumes only diffusional mass transfer and a constant hydrogen peroxide flux to the biofilm surface. Competition for hydrogen peroxide by the 10 μm diameter SECM tip at a distance of 100 μm away from the much larger biofilm surface is negligible.[56,57] Fitted hydrogen peroxide fluxes at the *V. fischeri* CB37 biofilm surfaces were found to be 2.5×10^{-10} mol/cm^2 s for 1 h incubation (lag phase) and 1.6×10^{-10} mol/cm^{2}s for the 4 h incubation (log phase). On the basis of a colony forming unit (CFU) count of 9.0×10^8 bacteria/mL, a 0.100 mL bacteria suspension aliquot, and a coverslip area of 2.54 cm^2, the calculated bacteria density was 3.5×10^7 bacteria/cm^2. Thus, approximately 7.1×10^{-18} mol (1 h incubation) and 4.5×10^{-18} mol (4 h incubation) of hydrogen peroxide were decomposed by a single *V. fischeri* CB37 bacterium at the biofilm surface per second. This further corresponds to ~4×10^6 and 3×10^6 molecules of hydrogen peroxide decomposed by a single *V. fischeri* CB37 bacterium at the biofilm surface per second, respectively, in keeping with the fact that catalase is known to be a perfect catalyst with a turnover number of 4×10^7 s^{-1} when the enzyme is saturated with a substrate (e.g., hydrogen peroxide).[58] Similarly, fitted hydrogen peroxide fluxes at the *V. fischeri* ETBB10-1 biofilm surfaces were found to be 0.9×10^{-10} mol/cm^2 s for 5 h incubation (first log phase), 1.8×10^{-10} mol/cm^{2}s for the 9 h incubation (second log phase), and 2.4×10^{-10} mol/cm^{2}s for the 12 h incubation (second semistationary phase). Thus, approximately 2.5×10^{-18} (5 h incubation), 5.2×10^{-18} (9 h incubation), and 6.9×10^{-18} (12 h incubation) mol (i.e., ~2×10^6, 3×10^6, 4×10^6 molecules, respectively) of hydrogen peroxide were decomposed by a single *V. fischeri* ETBB10-1 bacterium at the biofilm surface per second. These calculations provide an important estimate of the amount of hydrogen peroxide decomposed at the bacterial surface, which may be useful in understanding the defense mechanism of a particular bacterial species or interactions with a host in terms of metabolite or external hydrogen peroxide concentration.

Enhanced Catalase Activity in Response to Oxidative Stress. A number of planktonic bacteria (e.g., *H. influenza*,[59] *E. coli*,[30] *V. fischeri*,[22] *V. rumoiensis* S-1T,[26−28] *Aggregatibacter actinomycetemcomitans*[60]) have been shown to respond to the presence of hydrogen peroxide in their external environment by inducing catalase gene expression with a resulting increase in catalase activity. We therefore also used SECM to explore whether the free-living *V. fischeri* CB37 and symbiotic ETBB10-1 biofilms show increased catalase activity in response to external hydrogen peroxide in the culture media. Biofilms were exposed to low concentrations of hydrogen peroxide during early log phase growth (i.e., at 4 h incubation) and catalase activity was measured 1 h after introducing hydrogen peroxide into the growth media (i.e., at 5 h incubation). Hydrogen peroxide concentrations of 1 nM, 10 nM, and 10 μM were used in order to explore the lowest concentration needed to externally enhance catalase activity. These catalase activity results, in units of μmole hydrogen peroxide decomposed per minute, are shown by the solid blue dots in Figures 2B and 3B for *V. fischeri* CB37 and ETBB10-1 biofilms, respectively. Corresponding current vs time and peroxide concentration vs time plots are shown as Figure S7A,B in the Supporting Information for *V. fischeri* ETBB10-1 and Figure S8A,B in the Supporting Information for *V. fischeri* CB37. For the *V. fischeri* ETBB10-1 biofilms, catalase activity was enhanced at 5 h incubation from 0.15 ± 0.03 μmol H_2O_2/min (i.e., no hydrogen peroxide added during incubation) to 0.28 ± 0.01 (10 μM H_2O_2), 0.30 ± 0.01 (10 nM H_2O_2), and 0.32 ± 0.03 (1 nM H_2O_2) μmol H_2O_2/min, suggesting a similar level of catalase gene expression at the three concentrations. The average activity (0.30 ± 0.02 μmol H_2O_2/min) due to external induction at these hydrogen peroxide concentrations as shown in Figure 3B represents an approximately 2-fold increase in catalase activity compared to the 5 h incubation in the absence of hydrogen peroxide. Figure S7A,B in the Supporting Information shows that the activity of the externally induced *V. fischeri* ETBB10-1 biofilm approaches that of the biofilm incubated for 12 h. For the *V. fischeri* CB37 biofilms induced with 10 μM hydrogen peroxide, catalase activity was also enhanced at 5 h incubation to 0.35 ± 0.01 μmol H_2O_2/min (10 μM H_2O_2) compared to 0.24 ± 0.01 μmol H_2O_2/min at 4 h incubation and 0.23 ± 0.01 μmol H_2O_2/min at 6 h incubation. Figure S8A,B in the Supporting Information shows that the activity of the externally induced *V. fischeri* CB37 biofilm approaches that of the biofilm incubated for 9 h. These results indicate that catalase activity is enhanced in free-living *V. fischeri* CB37 and symbiotic *V. fischeri* ETBB10-1 biofilms in response to the presence of hydrogen peroxide in their external environment. On the basis of reported studies of gene regulation and protein expression in planktonic *V. fischeri* as discussed previously,[22] it is likely that the catalase activity enhancement measured in the biofilms reported here is a result of catalase gene expression. The results also suggest that the catalase activity enhancement in response to oxidative stress occurs by a similar mechanism in both the *V. fischeri* free-living CB37 and symbiotic ETBB10-1 biofilms. This suggests that *V. fischeri* bacteria, regardless of whether they are capable of colonizing squid light organs or never see such an environment, rely on high catalase activity and production when in a biofilm. Since biofilms are usually under selective pressures to maintain their integrity due to biotic forces such as grazing by predators, catalase activity may provide one avenue to prevent breakdown and deter bacteriovores from breaking down the complex biofilm community.[61] Such preventative measures are costly but are important for preventing a breach in the biofilm structure.

■ CONCLUSIONS

Using SECM, we monitored the decomposition of 1 mM hydrogen peroxide over the surface of *V. fischeri* biofilms in real time, related catalase activity to micromoles of hydrogen peroxide decomposed over 348 s, and showed that catalase activity depends on the incubation time of the biofilms in comparison with the respective planktonic bacteria growth curves. Examination of biofilms of both free-living and symbiotic *V. fischeri* strains revealed that the average catalase activity of these biofilms was similar for the same incubation times and growth conditions but differing planktonic growth curve behavior. Calculations based on Comsol Multiphysics simulations demonstrated that approximately $(3 \pm 1) \times 10^6$ molecules of hydrogen peroxide were decomposed by a single bacterium at a *V. fischeri* biofilm surface per second, suggesting efficient catalase activity when compared with reported

dx.doi.org/10.1021/ac402475m | *Anal. Chem.* 2014, 86, 498−505

turnover numbers on the order of 10^7 s^{-1} for isolated catalases in general when saturated with a substrate such as hydrogen peroxide. We also used SECM to explore catalase activity in response to external hydrogen peroxide in the growth media and showed up to a 2-fold enhancement in catalase activity at hydrogen peroxide induction concentrations as low as 1 nM and similar catalase activity enhancement in the free-living and symbiotic biofilms. Collectively, these quantitative, real time, and *in situ* catalase activity investigations on *V. fischeri* biofilms by SECM provide hydrogen peroxide spatial, temporal, and decomposition rate data that were not possible from earlier studies of bacteria in liquid culture or bacteria cell extracts. These studies also provide insight into the efficiency of the catalase activity of *V. fischeri* biofilms which is important in combatting the imposition of oxidative stress either through control of oxygen or imposition of hydrogen peroxide by the squid during colonization. The similar catalase activity found for biofilms of symbiotic and free-living *V. fischeri* bacteria suggests that a high level of catalase activity and production may be important in maintaining the integrity of these biofilms, regardless of whether the bacteria are capable of colonizing squid light organs. Further quantitative investigation of the mechanisms that control metabolic and external hydrogen peroxide concentrations with other strains of symbiotic and free living *V. fischeri* will lead to a better understanding of the role of catalase activity in symbiotic bacteria during colonization.

■ ASSOCIATED CONTENT

Supporting Information

Electrochemistry and hydrogen peroxide concentration data; Comsol Multiphysics simulation model and description. This material is available free of charge via the Internet at http://pubs.acs.org.

■ AUTHOR INFORMATION

Corresponding Author

*Fax: 575-646-2649. Phone: 575-646-5292. E-mail: czoski@nmsu.edu.

Notes

The authors declare no competing financial interest.

■ ACKNOWLEDGMENTS

The financial support of the National Science Foundation (Grant CHE-0809966 to C.G.Z) and a New Mexico State University Interdisciplinary Research Grant (C.G.Z., PI; M.K.N., Co-PI) are gratefully acknowledged. C.G.Z. thanks Prof. S. Lusetti and her group members Dr. L. Uranga and I. Menikpurage for valuable discussion and assistance with microbiology methodology and biochemical principles. CFU counts provided by N. Nourabadi and preliminary experiments by W. Castle and A. Devasurendra are acknowledged.

■ REFERENCES

(1) McFall-Ngai, M.; Heath-Heckman, E. A. C.; Gillette, A. A.; Peyer, S. M.; Harvie, E. A. *Sem. Immunol.* **2012**, *24*, 3−8.
(2) Rader, B. A.; Nyholm, S. V. *Biol. Bull.* **2012**, *223*, 103−111.
(3) Bosch, T. C. G.; McFall-Ngai, M. J. *Zoology* **2011**, *114*, 185−190.
(4) Visick, K. L.; Ruby, E. G. *Curr. Opin. Microbiol.* **2006**, *9*, 1−7.
(5) Ruby, E. G. *Nature* **2008**, *6*, 752−762.
(6) Ruby, E. G. *Annu. Rev. Microbiol.* **1996**, *50*, 591−624.
(7) Nishiguchi, M. K.; DeVinney, R.; Hirsch, A. M.; Riley, M.; Mansky, L.; Vendatum, G. *Vie Milieu* **2008**, *58*, 87−106.
(8) Chavez-Dozal, A. A.; Hogan, D.; Gorman, C.; Quintanal-Villalonga, A.; Nishiguchi, M. K. *FEMS Microbiol. Ecol.* **2012**, *81*, 562−573.
(9) Nyholm, S. V.; Nishiguchi, M. K. *Vie Milieu* **2008**, *58*, 175−184.
(10) Jones, B. W.; Nishiguchi, M. K. *Mar. Biol.* **2004**, *144*, 1151−1155.
(11) Graf, J.; Ruby, E. G. *Abst. Annu. Meeting Am. Soc. Microbiol.* **1994**, *94*, 76.
(12) Pennisi, E. *Science* **2013**, *340*, 1159−1160.
(13) Archetti, M.; Ubeda, F.; Fudenberg, D.; Green, J.; Pierce, N. E.; Yu, D. W. *Am. Nat.* **2011**, *177*, 75−85.
(14) Archetti, M. *J. Theor. Biol.* **2011**, *269*, 201−207.
(15) Schleicher, T. R.; Nyholm, S. V. *PLoS One* **2011**, *6*, e25649−e25649.
(16) Visick, K. L.; McFall-Ngai, M. *J. Bacteriol.* **2000**, *182*, 1779−1787.
(17) Ruby, E. G.; McFall-Ngai, M. J. *Trends Microbiol.* **1999**, *7*, 414−420.
(18) Small, A. L.; McFall-Ngai, M. J. *J. Cell. Biochem.* **1999**, *72*, 445−457.
(19) Nishiguchi, M. K. *Microbiol. Ecol.* **2002**, *44*, 10−18.
(20) Castillo, M. G.; Goodson, M. S.; McFall-Ngai, M. J. *Dev. Comp. Immunol.* **2009**, *33*, 69−76.
(21) Small, A. L.; McFall-Ngai, M. J. *J. Cell Biochem.* **1999**, *72*, 445−457.
(22) Visick, K. L.; Ruby, E. G. *J. Bacteriol.* **1998**, *180*, 2087−2092.
(23) Cosgrove, K.; Coutts, G.; Jonsson, I.-M.; Tarkowski, A.; Kokai-Kun, J. F.; Mond, J. J.; Foster, S. J. *J. Bacteriol.* **2007**, *189*, 1025−1035.
(24) Katsuwon, J.; Anderson, J. *Can. J. Microbiol.* **1992**, *38*, 1026−1032.
(25) Kim, K. K.; Fravel, D. R.; Papavizas, G. C. *Phytopathology* **1978**, *78*, 488−492.
(26) Ichise, N.; Hirota, K.; Ichihashi, D..; Nodasaka, Y.; Morita, N.; Okuyama, H.; Yumoto, I. *J. Biosci. Bioeng.* **2008**, *106*, 39−45.
(27) Yumoto, I.; Ichihashi, D.; Iwata, H.; Istokovics, A.; Ichise, N.; Matsuyama, H.; Okuyama, H.; Kawasaki, K. *J. Bacteriol.* **2000**, *182*, 1903−1909.
(28) Ichise, N.; Morita, N..; Hoshino, T.; Kawasaki, K.; Yumoto, I.; Okuyama, H. *Appl. Environ. Microbiol.* **1999**, *65*, 73−79.
(29) Ramsey, M. M.; Whiteley, M. *Proc. Natl. Acad. Sci. U.S.A.* **2009**, *106*, 1578−1583.
(30) Imlay, J. A. *Nature* **2013**, *11*, 443−454.
(31) McCarthy, B. J.; Hinshelwood, S. C. *Proc. R. Soc. London, Ser. B: Biol. Sci.* **1958**, *150*, 13−23.
(32) Li, Y.; Schellhorn, H. E. *J. Biomol. Tech.* **2007**, *18*, 185−187.
(33) Beers, R. F., Jr.; Sizer, I. W. *J. Biol. Chem.* **1952**, *195*, 133−140.
(34) Rorth, M.; Jensen, P. K. *Biochim. Biophys. Acta* **1967**, *139*, 171−173.
(35) Katsev, A. M.; Wegrzyn, G.; Szpilewska, H. *J. Basic Microbiol.* **2004**, *44*, 178−184.
(36) Bard, A. J.; Mirkin, M. V., Eds. *Scanning Electrochemical Microscopy*, 2nd ed.; CRC Press: New York, 2012.
(37) Fan, F. R. F.; Fernandez, J. L.; Liu, B.; Mauzeroll, J. In *Handbook of Electrochemistry*; Zoski, C. G., Ed. Elsevier: Amsterdam, The Netherlands, 2007; Chapter 12, pp 471−540.
(38) Bard, A. J. In *Scanning Electrochemical Microscopy*, 2nd ed.; Bard, A. J., Mirkin, M. V., Eds.; CRC Press: New York, 2012; Chapter 1, pp 1−14.
(39) Wang, X.; Yang, T.; Feng, Y.; Jiao, K.; Li, G. *Electroanalysis* **2009**, *21*, 819−825.
(40) Mao, L.; Osborne, P. G.; Yamamoto, K.; Kato, T. *Anal. Chem.* **2002**, *74*, 3684−3689.
(41) Liu, X.; Zweier, L. *Free Radical Biol. Med.* **2001**, *31*, 894−901.
(42) Horrocks, B. R.; Schmidtke, D.; Heller, A.; Bard, A. J. *Anal. Chem.* **1993**, *65*, 3605−3614.
(43) Wittstock, G.; Schuhmann, W. *Anal. Chem.* **1997**, *69*, 5059−5066.
(44) Wilhelm, T.; Wittstock, G. *Angew. Chem., Int. Ed.* **2003**, *24*, 2248−2250.

(45) Mezour, M. A.; Cornut, R.; Husssien, E. M.; Morin, M.; Mauzeroll, J. *Langmuir* **2010**, *26*, 13000−13006.
(46) Fan, F. R. F. In *Scanning Electrochemical Microscopy*, 2nd ed.; Bard, A. J., Mirkin, M. V., Eds.; CRC Press: New York, 2012; Chapter 4, pp 53−74.
(47) Mauzeroll, J.; Schougaard, S. B. In *Scanning Electrochemical Microscopy*, 2nd ed.; Bard, A. J., Mirkin, M. V., Eds.; CRC Press: New York, 2012; Chapter 12, pp 379−415.
(48) Beaulieu, I.; Juss, S.; Mauzeroll, J.; Geissler, M. *Anal. Chem.* **2011**, *83*, 1485−1492.
(49) Armemiya, S.; Guo, J.; Xiong, H.; Gross, D. A. *Anal. Bioanal. Chem.* **2006**, *386*, 458−471.
(50) Liu, X.; Ramsey, M. M.; Chen, X.; Koley, D.; Whiteley, M.; Bard, A. J. *Proc. Natl. Acad. Sci. U.S.A.* **2011**, *108*, 2668−2673.
(51) Koley, D.; Ramsey, M. M.; Bard, A. J.; Whiteley, M. *Proc. Natl. Acad. Sci. U.S.A.* **2011**, *108*, 19996−20001.
(52) Kuss, S.; Polcari, D.; Geissler, M.; Brassard, D.; Mauzeroll, J. *Proc. Natl. Acad. Sci. U.S.A.* **2013**, *110*, 9249−9254.
(53) Fan, F.-R. F; Demaille, C. In *Scanning Electrochemical Microscopy*, 2nd ed.; Bard, A. J., Mirkin, M. V., Eds.; CRC Press: New York, 2012; Chapter 3, pp 25−51.
(54) Fan, F. R. F.; Fernandez, J. L.; Liu, B.; Mauzeroll, J.; Zoski, C. G. In *Handbook of Electrochemistry*; Zoski, C. G., Ed.; Elsevier: Amsterdam, The Netherlands, 2007; Chapter 6, pp 189−199.
(55) Katsev, A. M.; Wegrzyn, G.; Szpilewska, H. *J. Basic Microbiol.* **2004**, *44*, 178−184.
(56) Zoski, C. G.; Aguilar, J. C.; Bard, A. J. *Anal. Chem.* **2003**, *75*, 2959−2966.
(57) Zoski, C. G.; Luman, C. R.; Fernandez, J. L.; Bard, A. J. *Anal. Chem.* **2007**, *79*, 4957−4966.
(58) Nelson, D. L.; Cox, M. M. *Principles of Biochemistry*, 5th ed.; W. H. Freeman and Co.: New York, 2008; Chapter 6, pp 183−233.
(59) Bishai, W. R.; Smith, H. O.; Barcak, G. J. *J. Bacteriol.* **1994**, *176*, 2914−2921.
(60) Brown, S. A.; Whiteley, M. *J. Bacteriol.* **2007**, *189*, 6407−6414.
(61) Chavez-Dozal, A. A.; Gorman, C.; Erken, M.; Steinberg, P. D.; McDougald, D.; Nishiguchi, M. K. *Appl. Environ. Microbiol.* **2013**, *79*, 553−558.